# RSC Advances

ROYAL SOCIETY OF CHEMISTRY

www.rsc.org/advances

Graphical Abstract:

# Highly efficient reversible adsorption of NO$_2$ in imidazole sulfonate room temperature ionic liquids

By Gang Yuan, Feng Zhang, Jiao Geng* and You-Ting Wu*

The molecular-imprinting like highly efficient reversible absorption of NO$_2$ in the imidazole sulfonate room-temperature ionic liquids, which opens a new way to clean the polluted air and re-utilize the wasted energy in nitrogen oxides.
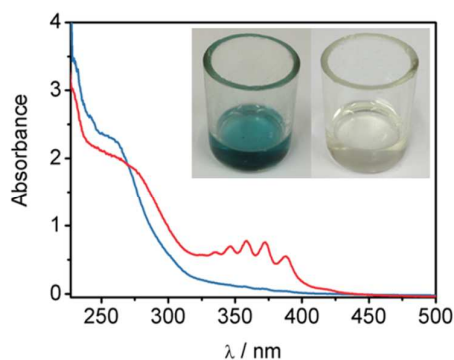
# Communication

# Highly efficient reversible adsorption of NO₂ in imidazole sulfonate room temperature ionic liquids

**Gang Yuan, Feng Zhang, Jiao Geng\* and You-Ting Wu\***

**The highly efficient reversible adsorption of NO₂ in room-temperature ionic liquids is reported for the first time, making a ground platform for promising applications.**

Controllable dissolution of nitrogen oxides (NO$_x$) is of great
10 importance for the design and application of hypergolic fuel,
organic synthesis (such as oxidation, nitration and nitrosation),[1-4]
and NO$_x$ sensing.[5] As a main source of air pollution, NO$_x$
contains huge amount of wasted energy which is difficult to be
reused.[6] Though species as NO₂ and N₂O₄ have been theoretically
15 proved to be ideal oxidizer,[7] it is problematic in handling and
application,[2,8] unless they are easily stored and reacted as our
wishes. Here, imidazole sulfonate ionic liquids (ILs) were found
to be ideal solvent for NO₂, and, what's more, the adsorption of
NO₂ in such ILs was reversible upon simple operations. The
20 study of such reversible adsorption process provides not only a
highly efficient method to separate NO₂, but also a promising and
fascinating way to utilize the wasted energy in NO$_x$.

With the advantages of ideal interfacial properties, negligible
vapor pressure, thermal stability, favorable viscosity, miscibility
25 with water and organic solvents, good abilities to extract metal
ions and compounds, and very friendly to the environment,[9-13]
ILs have been used in fields such as separation, bioanalytical
preconcentration and detection, organic synthesis, and
catalysis.[14-19] Therefore, there has been an explosion of interest in
30 the research of ionic liquids in recent years.[13] The capture or
sensing of gasses as N₂, CO₂, SO₂, and NO₂ in ILs has been
studied,[5,20-24] however, to the best of our knowledge, the
reversible adsorption of NO₂ and the interaction between cations
and NO₂ or N₂O₄ molecule in ILs has not been reported yet,
35 although such process is of huge application potential in the fields
as synthesis and energy utilization.

In our study, the imidazole sulfonate room-temperature ILs
including 1-ethyl-3-methylimidazolium trifluoromet-
hanesulfonate ([Emim]OTf), 1-butyl-3-methylimidazolium
40 trifluoromethanesulfonate ([Bmim]OTf), and 1-hexyl-3-
methylimidazolium trifleoromethanesulfonate ([HMIM]O-TF)
were chosen to be the solvent. The reversible adsorptions of NO₂
in these room-temperature ILs were found, respectively. In
addition, N₂O₄ was produced after the adsorption in each IL.
45 As shown in Figure 1, for [Hmim]OTf, the color of the
solution turned cyan blue after the adsorption of NO₂ at the
pressure of 40 kPa and the temperature of 35 °C (Fig. 1, insert
left). Compared with the UV-vis adsorption spectrum of

[Hmim]OTf (Fig. 1, blue line), six hyperfine split peaks at the
50 wavelengths of 324.6 nm, 335.3 nm, 346.0 nm, 358.8 nm, 372.2
nm, and 387.9 nm, respectively, appeared after the adsorption
(Fig. 1, red line), resulting from the vibrational electronic
transition of N₂O₄.[25-28] The same color change appeared with
[Emim]OTf and [Bmim]OTf after adsorbing NO₂ at the same
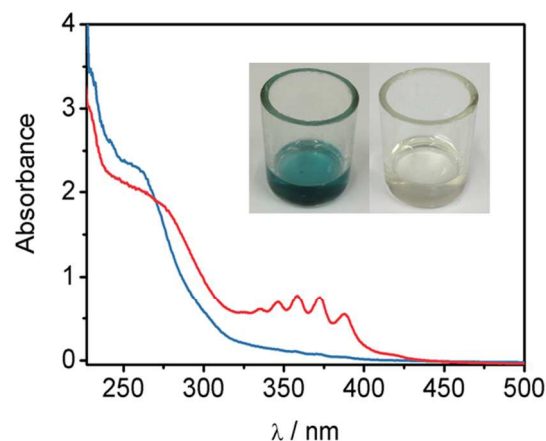55 condition.



**Fig. 1** UV-vis spectra of [Hmim]OTf before (blue line) and after (red line) adsorption of NO₂. Insert: the photograph of [Hmim]OTf with NO2 in it (left) and after release of NO₂ (right). The adsorption pressure was 40 kPa.

However, different from [Hmim]OTf and [Bmim]OTf, a new
60 peak at 417.0 nm appeared on the spectrum of [Emim]OTf after
adsorbing NO₂ as well as the six fine peaks (Fig. 1 and S1 in
ESI†), which should be ascribed to the UV-vis adsorption of NO₂
monomer.[26-28] The great tendency of NO₂ monomer to become
the dimer led to the formation of N₂O₄. Meanwhile, the structure
65 of π bond of N₂O₄ is prone to form $\pi_{cation}$-π interaction with
imidazole cation in the ILs,[29] which could be a main factor
contributed to the adsorption state of NO₂ in these ILs. The cyan
blue color was probably due to the $\pi_{cation}$-π interaction and the ion
interaction induced charge transfer. The disintegration of N₂O₄
70 was easier among the molecules of [Emim]OTf than in the other
two ILs, since the smaller steric hindrance of alkyl on
[Emim]OTf make room for the stronger molecular motion of
N₂O₄. Therefore, the ratio of NO₂ monomer was bigger in
[Emim]OTf than in [Bmim]OTf and [Hmim]OTf, leading to the
75 obvious additional adsorption peak at the wavelength of 417.0 nm
(Fig. S1a in ESI†). This fact also referred that the six split peaks
around 320-390 nm attributed most to N₂O₄.

The fourier transform infrared (FTIR) spectra of [Emim]OTf, [Bmim]OTf, and [Hmim]OTf were recorded before and after the adsorption of $NO_2$, respectively (Fig. S2 in ESI†). After the adsorption of $NO_2$, a new transmission peak at 1665 $cm^{-1}$ was
5 recorded with [Emim]OTf and [Bmim]OTf, respectively (Fig. S2a and S2b in ESI†). Meanwhile, for [Hmim]OTf the new peak appeared at 1662 $cm^{-1}$. These peaks should be ascribed to the a-stretch vibration of $N_2O_4$.[30] The slight red-shift of IR adsorption in [Hmim]OTf was probably because that the inductive effect and
10 the steric hindrance of –hexyl constrained the a-stretch vibration, leading to the vibration strength. While the same effect of –ethyl and –butyl were not as strong as –hexyl. Accompany with the UV-vis spectra, the FTIR spectra (Fig. S2 in ESI†) confirmed the existence of $N_2O_4$, indicating the successful adsorption and
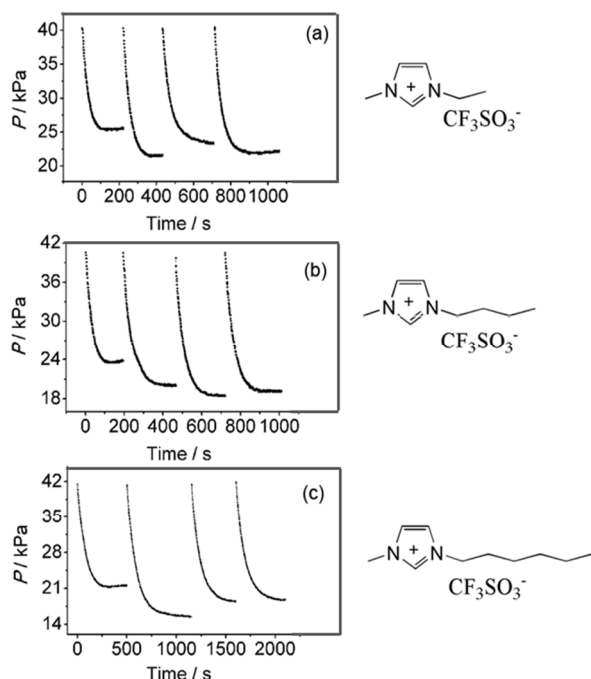15 stabilization of $NO_2$ by the imidazole sulfonate ILs.



**Fig. 2** The pressure change upon the adsorption-desorption cycles of $NO_2$ in [Emim]OTf (a), [Bmim]OTf (b), and [Hmim]OTf (c) at 35 °C. Insert is the structural formula of each IL.

With the help of $\pi_{cation}$-$\pi$ interaction between $N_2O_4$ and the
20 imidazole sulfonate IL molecules, the adsorbed $N_2O_4$ could remain stable in these ILs in the closed container. After 2 months, the colors of the solutions still remained unchanged. Once open to the air at 25 °C, $NO_2$ will gradually release from the solvent. The color of the solution turned from dark cyan blue to yellow
25 and to transparent eventually. The time of release depends on the solvent. Generally, in [Emim]OTf, it spent about 2 hours, in [Bmim]OTf it was 5 hours, and 20 hours for [Hmim]OTf, indicating reversible adsorption-desorption properties.

To investigate the reversible adsorption-desorption process,
30 vacuum conditions were applied so that the $N_2O_4$ and $NO_2$ dissolved in the ILs could release immediately. Two containers (one for gas storage and the other for adsorption) were connected together with a valve. A vacuum pump and a pressure sensor were also connected to the system so that the gas pressure could
35 be controlled. At the initial pressure of $NO_2$ as 40 kPa, the

adsorption processes were conducted in 4 g [Emim]OTf, [Bmim]OTf, and [Hmim]OTf, respectively. With the help of vacuum-assisted desorption, pressure changes during 4 cycles of adsorption-desorption processes in each IL were recorded as
40 shown in Fig. 2. The pressures of the connected system, which was positively related to the remained amount of $NO_2$, decreased rapidly indicating the fast adsorption of $NO_2$ in these ILs. The adsorption equilibrium achieved after about 100 s in [Emim]OTf and [Bmim]OTf (Fig. 1a and 1b), respectively, and 280 s in
45 [Hmim]OTf (Fig. 1c). The longer adsorption time in [Hmim]OTf probably resulted from the bigger steric hindrance of –hexyl on HMIM molecule than –ethyl on EMIM and –butyl on BMIM (Fig. 1, insert), which made it more difficult for $NO_2$ to enter the space among [Hmim]OTf molecules and located on the best adsorption
50 site.

During the second adsorption round, the equilibrium achieved later compared with the first one in all the ILs. It spent about 130 s in [Emim]OTf (Fig. 1a), 175 s in [Bmim]OTf (Fig. 1b), and 450 s in [Hmim]OTf (Fig. 1c), respectively. Meanwhile, more $NO_2$
55 was adsorbed in each IL, which was probably because the adsorbed $NO_2$ in the first adsorption-desorption process made path and room in IL molecules for the followed $NO_2$ molecules, just like what happens in molecular imprinting. The more amount of $NO_2$ adsorption led to the longer adsorption time in each IL.
60 As shown in Fig. 1, the molecular-imprinting like processes achieved their equilibriums at 360 s in [Emim]OTf (the second adsorption-desorption round), 630 s in [Bmim]OTf (the third round), and 900 s in [Hmim]OTf (the second round), respectively, showing that the bigger the steric hindrance of alkyl group on the
65 imidazole cation, the longer the imprinting time was. This fact, together with the FTIR results, indicates that the adsorption of $NO_2$ (taking form of dimer) was through the interaction with the imidazole parts of ILs. After the imprinting process, some of $NO_2$ molecules were deeply adsorbed by the ILs and could not be
70 driven out by simply applying vacuum condition, so that they could not be replaced by the $NO_2$ molecules in the next round. Therefore, the adsorption amount of $NO_2$ decreased in the next adsorption round, but still more than the first round without the molecular-imprinting like process.
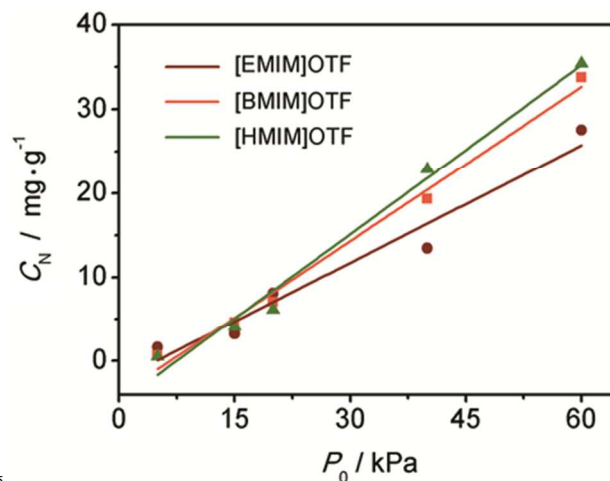


**Fig. 3** The relationship between the amount of $NO_2$ adsorbed in unit gram of IL ($C_{NO2}$), in different ILs (left corner), and the initial pressure ($P_0$)

Both of the pressure changes in the adsorption-desorption

processes and the molecular-imprinting like processes illustrate that the adsorption of $NO_2$ in the imidazole sulfonate ILs is reversible and controllable, unlike in water and the other solvents. The solubility of $NO_2$ in each IL was evaluated at different initial pressures. There is the linear relationship between the dissolved amount of $NO_2$ in unit gram of IL ($C_{NO2}$, Calculated from the pressure change shown in Fig. S3 in ESI†) and the initial pressure ($P_0$), which is $P_0 = 0.46 C_{NO2} - 2.28$ ($R^2=0.95$) in [Emim]OTf; $P_0 = 0.61 C_{NO2} - 4.05$ ($R^2=0.99$) in [Bmim]OTf; and $P_0 = 0.67 C_{NO2} - 5.00$ ($R^2=0.98$) in [Emim]OTf, respectively (Fig. 3). The good but simple linear ship is in accordance with Henry's Law, indicating the inexistence of complex chemical reactions the solute and the solvent during the adsorption. Additionally, the average amount of $NO_2$ adsorbed in these three ILs at 60 kPa was 32.2 mg g$^{-1}$, which means 15.7 mL $NO_2$ at the standard state could be adsorbed into 1 g solvent.

Besides, the reversible adsorption of $NO_2$ in the ILs was studied with the temperature changing from 35 °C to 65 °C. With the initial pressure of 42 kPa, the solubility of $NO_2$ in the ILs decreased as the temperature grew up (Fig. S4 in ESI†). The equilibrium pressure at 45 °C, 55 °C, and 65 °C were almost the same in [Emim]OTf (Fig. S4a in ESI†), but different from each other in [Bmim]OTf and [Hmim]OTf, especially in the latter (Fig. S4b and S4c). Moreover, the equilibrium pressures at 65 °C in the three ILs were almost the same (Fig. S4 in ESI†, 29.3 kPa for [Emim]OTf, 31.4 kPa for [Bmim]OTf, and 30.9 kPa for [Hmim]OTf). The different variation rate of the equilibrium pressures towards the temperature in the different IL is proposed to be resulted from the different molecular motion of $N_2O_4$ in each IL. In [Emim]OTf, the steric hindrance is smaller than the other two solvents, leading to the smaller inter-molecular fraction. Therefore, the frequency and strength of the motion of $N_2O_4$ molecules in [Emim]OTf increased rapidly as the temperature grew up, which is in accordance with the UV-vis spectrum (Fig. S1 in ESI†, the extra peak appeared at 417.0 nm). As a result, the internal energy of the $N_2O_4$-[Emim]OTf increased rapidly, which means the adsorption enthalpy change (ΔH) increased rapidly with the temperature growth. Thus the adsorption equivalent shifted to the left rapidly, leading to the rapid equilibrium-pressure growth with the temperature growth. On the other hand, in [Hmim]OTf the bigger hindrance led to the slower changing rate of the reaction enthalpy, so that the equilibrium pressure grew slower. As the temperature grew, the increase of the frequency and strength of $N_2O_4$ molecular motion gradually slowed down, since the bigger constraint resulting from the molecular body of each IL. Therefore the motion in different IL eventually tended to be almost the same level, leading to nearly the same equilibrium pressures in three ILs at 65 °C. In addition, $NO_2$ exists in equilibrium with the colourless $N_2O_4$ as an exothermic process with enthalpy change of about -57 kJ/mol.[31,32] $NO_2$ will be favoured at high temperatures. This single equilibrium existed in all of the three ILs, thus did not interfere with the change of equilibrium pressures. The temperature related adsorption proves the proposed adsorbing mechanism again and provides important data for the application in the scenes of real work.

To sum up, $NO_2$ can be reversibly adsorbed in imidazole sulfonate room temperature ILs and takes form of dimer among IL molecules. Unlike in water and the other solvents, the molecular-imprinting like process was found during the adsorption-desorption cycles in these ILs. The solubility of $NO_2$ in different ILs depends on the initial pressure, temperature, and the steric hindrance of alkyl on imidazole cation. The well adsorbed $NO_2$ can be conveniently used in the fields like fuel cell design and the possible organic synthesis, which opens a new way to separate and utilize the wasted energy in nitrogen oxides. We believe these initial results will make our life cleaner and the energy be utilized more efficiently in varieties of chemical industries.

## Notes and references

$^a$ *Department of Chemical Engineering, School of Chemistry and Chemical Engineering, Nanjing University, Nanjing 210093, P. R. China. Fax: +86 25 83595559; Tel: +86 25 83595559; E-mail: gengjiao@nju.edu.cn; ytwu@nju.edu.cn*

1 W. G. Liu and W. A. Goddard, *J. Am. Chem. Soc.,* 2012, **134**, 12970–12978.
2 C. Nonnenberg, I. Frank and T. M. Klapotke, *Angew. Chem. Int. Ed.*, 2004, **43**, 4585–4589.
3 R. A. Pierce, R. P. Campbell-Kelly, A. E. Visser and J. E. Laurinat, *Ind. Eng. Chem. Res.*, 2007, **46**, 2372–2376.
4 A. Commeyras, H. Collet, L. Boiteau, J. Tailades, O. Vandenabeele-Trambouze, H. Cottet, J. P. Biron, R. Plasson, L. Mion, O. Lagrille, H. Martin, F. Selsis and M. Dobrijevic, *Polym. Int.*, 2002, **51**, 661–665.
5 R. Toniolo, N. Dossi, A. Pizzariello, A. P. Doherty and G. Bontempelli, *Electroanalysis*, 2012, **24**, 865–871.
6 L. N. Lamsal, R. V. Martin, D. D. Parrish and N. A. Krotkov, *Environ. Sci. Technol.*, 2013, **47**, 7855–7861.
7 Y. Liu, S. V. Zybin, J. Guo, A. C. T. van Duin and W. A. Goddard, *J. Phys. Chem. B*, 2012, **116**, 14136–14145.
8 P. Rumbach, M. Witzke, R. M. Sankaran and D. B. Go, *J. Am. Chem. Soc.*, 2013, **135**, 16264–16267.
9 L. B. Escudero, A. C. Grijalba, E. M. Martinis and R. G. Wuiloud, *Anal. Bioanal. Chem.,* 2013, **405**, 7597–7613.
10 L. B. Escudero, P. Berton, E. M. Martinis, R. A. Olsina and R. G. Wuiloud, *Talanta*, 2012, **88**, 277–283.
11 C. H. Xu, A. Durumeric, H. K. Kashyap, J. Kohanoff and C. Margulis, *J. Am. Chem. Soc.,* 2013, **135**, 17528–17536.
12 T. Welton, *Chem. Rev.*, 1999, **99**, 2071–2084.
13 K. R. J. Lovelock, I. J. Villar-Garcia, F. Maier, H. P. Steinrück and P. Licence, *Chem. Rev.,* 2010, **110**, 5158–5190.
14 T. Welton and J. P. Hallett, *Chem. Rev.*, 2011, **111**, 3508–3576.
15 D. S. Silvester, *Analyst*, 2011, **136**, 4871–4882.
16 W. Qian, E. Jin, W. Bao and Y. Zhang, *Angew. Chem. Int. Ed.*, 2005, **44**, 952.
17 D. B. G. Williams, M. Ajam and A. Ranwell, *Organometallics*, 2007, **26**, 4692.
18 N. V. Plechkova and K. R. Seddon, *Chem. Soc. Rev.*, 2008, **37**, 123.
19 C. F. Poole and S. K. Poole, *J. Chromatogr. A* 2010, **1217**, 2268–2286.
20 X. H. Huang, C. J. Margulis, Y. H. Li and B. J. Berne, *J. Am. Chem. Soc.*, 2005, **127**, 17842–17851.

21  C. Wang, G. Cui, X. Luo, Y. Xu, H. Li and S. Dai, *J. Am. Chem. Soc.*, 2011, **133**, 11916–11919.

22  S. M. Mahurin, T. Dai, J. S. Yeary, H. Luo and S. Dai, *Ind. Eng. Chem. Res.*, 2011, **50**, 14061–14069.

5 23  S. Ren, Y. Hou, W. Wu and M. Jin, *Ind. Eng. Chem. Res.*, 2011, **50**, 998–1002.

24  L. L. Zhang, J. X. Wang, Y. Xiang, X. F. Zeng and J. F. Chen, *Ind. Eng. Chem. Res.*, 2011, **50**, 6957–6964.

25  M. F. Merienne, A. Jenouvrier, B. Coquart and J. P. Lux, *J. Atmos. Chem.*, 1997, **27**, 219–232;

10 26  K. Yoshino, J. R. Esmond and W. H. Parkinson, *Chem. Phys.*, 1997, **221**, 169–174.

27  J. Orphal, *Photochem. Photobiol. A-Chem.*, 2003, **157**, 185–209.

28  J. N. Crowley and S. A. Carl, *J. Phys. Chem. A*, 1997, **101**, 4178–4184.

15 29  V. Georgakilas, M. Otyepka, A. B. Bourlinos, V. Chandra, N. Kim, K. C. Kemp, P. Hobza, R. Zboril and K. S. Kim, *Chem. Rev.*, 2012, **112**, 6156–6214.

30  H. Beckers, X. Zeng and H. Willner, *Chem. Eur. J.*, 2010, **16**, 1506–1520.

20 31  C. S. Sharov, E. A. Konstantinova, L. A. Osminkina, V. Y. Timoshenko and P. K. Kashkarov, *J. Phys. Chem. B*, 2005, **109**, 4684-4693.

32  J. Barin and O. Knacke, *Thermochemical Properties of Inorganic Sunstances*; Springer: Berlin, 1977.